

The first electron beam polarization measurement with a diamond micro-strip detector

A. Narayan¹, D. Dutta¹, V. Tvaskis^{2,3}, D. Gaskell⁴, J. W. Martin², A. Asaturyan⁵, J. Benesch⁴, G. Cates⁶, B. S. Cavness⁷, J. C. Cornejo⁸, M. Dalton⁶, W. Deconinck⁸, L. A. Dillon-Townes⁴, G. Hays⁴, E. Ihloff⁹, D. Jones⁶, R. Jones¹⁰, S. Kowalski¹¹, L. Kurchaninov¹², L. Lee¹², A. McCreary¹³, M. McDonald², A. Micherdzinska², A. Mkrтчyan⁵, H. Mkrтчyan⁵, V. Nelyubin⁶, S. Page³, K. Paschke⁶, W. D. Ramsay¹², P. Solvignon⁴, D. Storey², A. Tobias⁶, E. Urban¹⁴, C. Vidal⁹, P. Wang³, and S. Zhamkotchyan⁵

¹Mississippi State University, Mississippi State, MS 39762, USA

²University of Winnipeg, Winnipeg, MB R3B 2E9, Canada

³University of Manitoba, Winnipeg, MB R3T 2N2, Canada

⁴Thomas Jefferson National Accelerator Facility, Newport News, VA 23606, USA

⁵Yerevan Physics Institute, Yerevan, 375036, Armenia

⁶University of Virginia, Charlottesville, VA 22904, USA

⁷Angelo State University, San Angelo, TX 76903, USA

⁸College of William and Mary, Williamsburg, VA 23186, USA

⁹MIT Bates Linear Accelerator Center, Middleton, MA 01949, USA

¹⁰University of Connecticut, Storrs, CT 06269, USA

¹¹Massachusetts Institute of Technology, Cambridge, MA 02139, USA

¹²TRIUMF, Vancouver, BC V6T 2A3, Canada

¹³University of Pittsburgh, Pittsburgh, PA 15260, USA and

¹⁴Hendrix College, Conway, AR 72032, USA

A diamond multi-strip detector was used for the first time, to track Compton scattered electrons in a new electron beam polarimeter in experimental Hall C at Jefferson Lab. We report the first high precision beam polarization measurement with electrons detected in diamond multi-strip detectors. The analysis technique leveraged the high resolution of the detectors and their proximity to the electron beam ($\gtrsim 0.5$ cm). The polarization was measured with a statistical precision of $< 1\%$ /hr, and a systematic uncertainty of 0.59%, for a 1.16 GeV electron beam with currents up to 180 μ A. This constitutes the highest precision achieved for polarization measurement of few-GeV electron beams.

PACS numbers:

INTRODUCTION

High precision nuclear physics experiments using polarized electron beams rely on accurate knowledge of beam polarization to achieve their ever improving precision. A parity violating electron scattering (PVES) experiment in the experimental Hall C at Jefferson Lab (JLab), known as the Q_{weak} experiment, is the most recent example [1, 2]. The goal of the Q_{weak} experiment is to measure the Standard Model parameter known as the weak mixing angle, at a low energy (relative to the Z^0 mass) with unprecedented precision. With a goal of $< 1\%$ uncertainty, determination of electron beam polarization is one of the greatest technical challenges of the Q_{weak} experiment. The experiment utilized an existing Møller polarimeter [2, 3] and a new Compton polarimeter [2, 4] to monitor the electron beam polarization. The Compton polarimeter was the only polarimeter at JLab Hall C that could non-destructively monitor the beam polarization at very high beam currents. A novel aspect of this polarimeter was the first use of diamond detector technology for this purpose.

The use of *natural* diamond in the detection of charged particles and radiation has a long history; but the use of

synthetic diamond grown through a process known as “chemical vapor deposition” (CVD) is a relatively recent development. Detailed reviews of diamond as charged particle detectors can be found in [12–14]. Thin sheets of centimeter-sized diamond are grown using the CVD process and the plates of diamond are then turned into charged particle detectors by depositing suitable electrodes on them [15]. Compared to the more commonly used silicon detector, the signal size in a diamond detector is smaller, but the higher electron and hole mobility of diamond leads to a faster and shorter duration signal. However, the well-established radiation hardness of diamond [16, 17] is by far the most important consideration for the use of diamond detectors in nuclear and particle physics experiments.

The use of Compton scattered electrons and/or back-scattered photons to measure the Compton asymmetry and thereby the electron beam polarization, is a well established polarimetry technique [5–10]. Most previous Compton polarimeters, other than the one used in the SLD experiment [7], relied primarily on detection of the scattered photons to measure the beam polarization. The SLD Compton polarimeter, which detected scattered electrons (and used detection of photons as a cross-

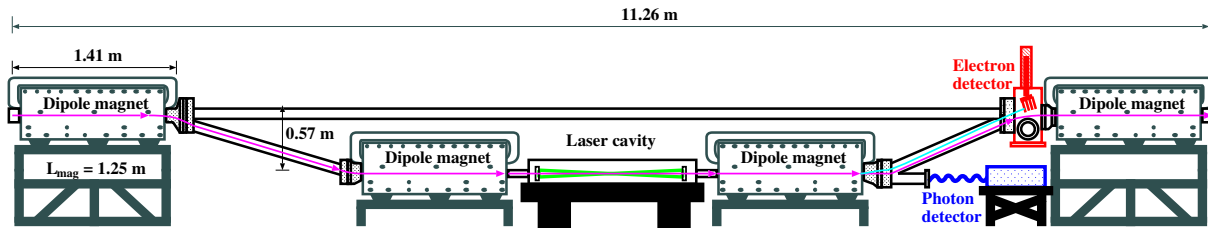


FIG. 1: Schematic diagram of the JLab Hall C Compton polarimeter. Four identical dipole magnets forming a magnetic chicane that displaces a 1.16 GeV electron beam vertically downward by 57 cm ($\sim 10.13^\circ$). An external low-gain Fabry-Pérot laser cavity provided a high intensity ($\sim 1 - 2$ kW) beam of $\sim 100\%$ circularly polarized green (532 nm) photons. The laser light is focused at the interaction region ($\sigma_{\text{waist}} \sim 90 \mu\text{m}$), and it is larger than the electron beam envelope ($\sigma_{x/y} \sim 40 \mu\text{m}$).

check), was operated at a beam energy of 50 GeV and reported a precision of 0.5%. The relatively low energy of the electron beam at JLab leads to a smaller Compton analyzing power, and makes it significantly more challenging to achieve the same level of precision. Nonetheless, the Compton polarimeter in Hall A at Jefferson Lab has reported a relative precision of $\sim 1\%$ by detecting the Compton scattered electrons at a beam energy of 3 GeV [11].

The low energy of the electron beam (1.16 GeV) and other operating parameters of the Q_{weak} experiment, presented the most challenging set of conditions to achieve the goal of $< 1\%$ uncertainty in measurement of the beam polarization. For example, it constrained the tracking detector to be placed as close as 0.5 cm from the electron beam. Further, the polarimeter was operated at the highest beam current (180 μA) ever used by any experiment at JLab and ran for over 5000 hrs, thereby subjecting the electron detectors to a rather large cumulative radiation dose (> 100 kGy, just from electrons). In order to withstand the large radiation dose, a novel set of diamond micro-strip detectors were used to track the scattered electrons in the JLab Hall C Compton polarimeter. In this letter we report the first high precision measurement of electron beam polarization with this device.

THE HALL C COMPTON POLARIMETER

A schematic of the Compton polarimeter in Hall C at JLab is shown in Fig. 1, and details can be found in Ref. [2, 4]. The Compton scattered electrons were momentum analyzed by the third dipole magnet of the chicane which bent the primary beam by $\sim 10.13^\circ$. The maximum separation between the primary electron beam and the Compton scattered electrons, just in front of the fourth dipole, was ~ 17 mm. The deflection of scattered electrons with respect to the primary electron beam, from the maximum down to distances as small as ~ 5 mm, was tracked by a set of four diamond micro-strip detectors. This range allowed the detection of a large fraction of the Compton electron spectrum, from

beyond the kinematic maximum (strip 55 in Fig. 3) past the zero-crossing point (~ 8.5 mm from the primary beam) of the Compton asymmetry. The electron detectors were made from 21 mm \times 21 mm \times 0.5 mm plates of CVD diamond [2]. Each diamond plate has 96 horizontal metalized electrode strips with a pitch of 200 μm (180 μm of metal and 20 μm of gap) on one side. Further details can be found in Ref. [2, 4]. A photograph of a single detector plane is shown in Fig 2.

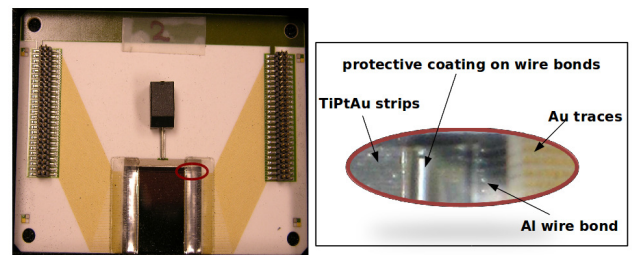


FIG. 2: A CVD diamond plate mounted on an alumina substrate which forms a single detector plane (left). The red oval indicates the area that has been shown in the enlarged view (right).

A Compton electron rate, aggregated over all strips in each detector plane, of $\sim 150 - 180$ kHz was observed with these detectors and the signal-to-background ratio was $\sim 5 - 20$ [2]. By comparing the expected to the observed rates, the detector efficiency was estimated to be $\sim 70\%$. The large separation between the detector and the readout electronics was the leading cause of the inefficiency.

The data acquisition (DAQ) system employed a set of field programmable gate array (FPGA) based logic modules to find clusters of detector hits, and to implement a track-finding algorithm, which generated a trigger when the same cluster was identified in multiple active planes. The cluster size was set to 4 adjacent strips. Only 3 detector planes were operational during the experiment and the typical trigger condition was set to 2 out of 3 planes.

Over the 2 year period of the Q_{weak} experiment, the detectors were exposed to a radiation dose of ~ 100 kGy

114 (without including the dose from Synchrotron radiation).
 115 No significant degradation of the signal size was observed
 116 during this period, demonstrating the radiation hardness
 117 of the diamond detectors.

118 DATA REDUCTION AND RESULTS

119 The electron beam helicity was reversed at a rate of
 120 960 Hz in a pseudo-random sequence. In addition a
 121 half-wave plate in the polarized electron photo emission
 122 source [18] was inserted or removed about every 8 hours
 123 to reverse the beam helicity relative to the polarization
 124 of the source laser.

125 The Compton laser was operated in ~ 90 second cy-
 126 cles (~ 60 s on and ~ 30 s off). The laser off data were
 127 used to measure the background. The background yield
 128 measured during the laser-off period was subtracted from
 129 the laser-on yield for each electron helicity state, and a
 130 charge normalized Compton yield for each detector strip
 131 was obtained for the two electron helicities. The mea-
 132 sured asymmetry was built from these yields using,

$$A_{exp} = \frac{Y^+ - Y^-}{Y^+ + Y^-}, \quad (1)$$

133 where $Y^\pm = \frac{N_{on}^\pm}{Q_{on}^\pm} - \frac{N_{off}^\pm}{Q_{off}^\pm}$ is the charge normalized Comp-
 134 ton yield for each detector strip, $N_{on/off}^\pm$ and $Q_{on/off}^\pm$
 135 are the detector counts and the beam charge accumu-
 136 lated during the laser on/off period for the two electron
 137 helicity states (\pm), respectively. A statistical precision
 138 of $< 1\%$ per hour was routinely achieved. The Comp-
 139 ton yields were integrated over two different time inter-
 140 vals, ~ 250 thousand helicity cycles and 1 laser cycle. The
 141 asymmetries extracted over both time intervals, and aver-
 142 aged over an hour long run, were consistent with one an-
 143 other. A typical spectrum for an hour long run is shown
 144 in Fig. 3. The background asymmetry is consistent with
 145 zero within the statistical uncertainties, and given the
 146 large signal-to-background ratio of 5–20, the dilution to
 147 the measured asymmetry due to the background is neg-
 148 ligible.

149 The electron beam polarization P_e was extracted by
 150 fitting the measured asymmetry to the theoretical Comp-
 151 ton asymmetry using;

$$A_{exp}(y_n) = P_e P_\gamma A_{th}(y_n), \quad (2)$$

152 where P_γ is the polarization of the photon beam, y_n is the
 153 scattered electron displacement along the detector plane
 154 for the n -th strip, and A_{th} is the $\mathcal{O}(\alpha)$ theoretical Comp-
 155 ton asymmetry for fully polarized electrons and photon
 156 beams. The radiative corrections to the Compton asym-
 157 metry were calculated to leading order within a low en-
 158 ergy approximation applicable for few GeV electrons [19].
 159 The relative change in the Compton asymmetry due to
 160 radiative corrections was $< 0.3\%$.

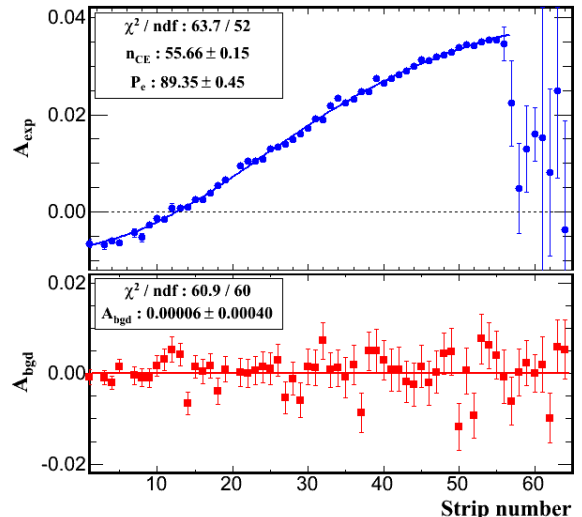


FIG. 3: The measured asymmetry as function of detector strip number for a single detector plane during the laser-on period (top) and the background asymmetry from the laser-off period (bottom). The strip number is linearly mapped to the displacement of the scattered electron from the primary beam. The solid blue line (top) is a fit to Eq. 2 and the solid red line (bottom) is a fit to a constant value. Only statistical uncertainties are shown in this figure.

The quantity A_{th} is typically calculated as a function of the dimensionless variable $\rho = E_\gamma / E_\gamma^{max}$, where E_γ and E_γ^{max} are the energy of the back-scattered photon and its maximum value, respectively. In order to directly compare with the measured asymmetry, ρ was mapped, by a third order polynomial, to the displacement of the scattered electron along the detector plane y_n . Further, y_n is linearly related to detector strip number, and depends on several parameters, such as, dimensions and dispersion of the chicane magnets, and exact location of the detectors with respect to the third dipole.

The measured asymmetry A_{exp} was fit to Eq. 2 for each detector strip, with P_e and n_{CE} (the strip number that detects the maximum displaced electrons) as the two free parameters. The number of degrees of freedom was typically between 50 – 60, which was made possible by the high resolution of the detector, and the proximity of the detector to the primary electron beam. The detection of a large fraction of the Compton electron spectrum, spanning both sides of the zero crossing of the Compton asymmetry, significantly improved the robustness of the fit and the analysis technique. A typical fit is shown in Fig. 3. The χ^2 per degree-of-freedom of the fit ranges between 0.8 – 1.5 for all production runs reported here.

A Monte Carlo (MC) simulation of the Compton polarimeter was coded in the GEANT3 [20] detector simulation package. In addition to Compton scattering, the simulation included backgrounds from beam-gas interactions and beam halo interactions in the chicane ele-

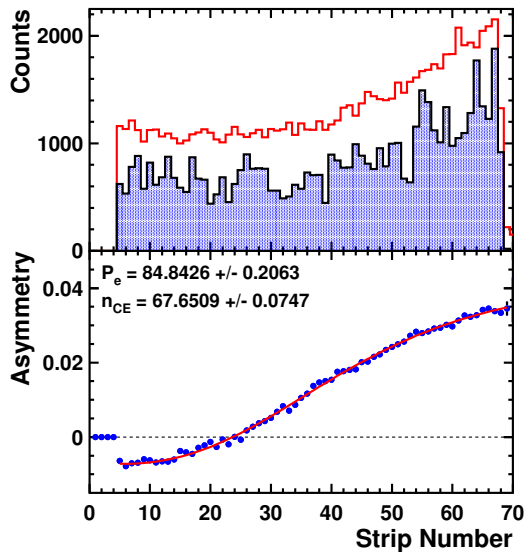


FIG. 4: (top) A typical Monte Carlo simulated Compton spectrum for a single detector plane, with (blue, shaded) and without (red) detector inefficiency. The counts have been scaled by a factor of 10^{-3} . (bottom) The Compton asymmetry extracted from the simulated spectrum including detector inefficiency (blue circles), and a two parameter fit to the calculated asymmetry (red line). The input asymmetry was 85%.

190 ments. The simulation also incorporated the effects of
 191 detector inefficiency, the track-finding trigger, and elec-
 192 tronic noise. A typical simulated strip-hit spectrum (with
 193 and without detector inefficiency), and the asymmetry
 194 extracted from simulated spectra are shown in Fig. 4.
 195 The simulation was used to validate the analysis pro-
 196 cedure and to study a variety of sources of systematic
 197 uncertainty. For each source, the relevant parameter was
 198 varied within the expected range of uncertainty, and the
 199 change in the extracted polarization was listed as its con-
 200 tribution to the systematic uncertainty. The list of con-
 201 tributions is shown in Table I.

202 The MC simulation demonstrated that secondary par-
 203 ticles knocked out by the Compton scattered electron
 204 passing through the first plane produced a 0.4% change
 205 in polarization in the subsequent planes, consistent with
 206 observation. A correction for the second and third planes
 207 could be made but at the cost of a slightly higher sys-
 208 tematic uncertainty, and hence only the results from the
 209 first detector plane are quoted here.

210 There were several sources of inefficiency associated
 211 with the DAQ system, such as the algorithm used to iden-
 212 tify electron tracks and form the trigger, and the dead-
 213 time due to a busy (hold off) period in the DAQ. The
 214 entire DAQ system was simulated on a platform called
 215 Modelsim [21]. While in Monte Carlo simulations, events
 216 are generated based on the probability distribution for
 217 the relevant physics process, in contrast Modelsim is a

218 simulation technique based on time steps. It employs
 219 the same firmware, written in the hardware description
 220 language for very high speed integrated circuits (VHDL),
 221 that operated the logic modules in the DAQ system. The
 222 DAQ simulation included signal generators that mimic
 223 the electron, the background and the noise signals, along
 224 with a detailed accounting of delays due to the internal
 225 signal pathways in the logic modules and the external
 226 electronic chain.

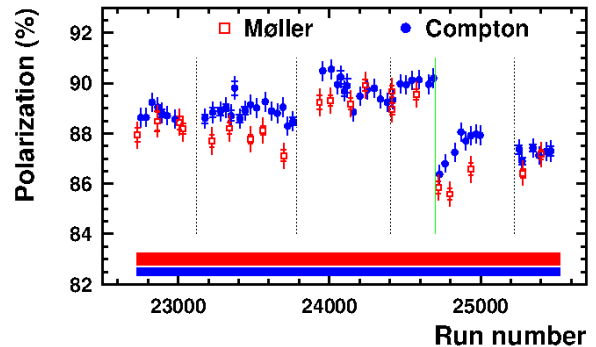


FIG. 5: The extracted beam polarization as a function of run-number averaged over 30 hour long periods, during the second run period of the Q_{weak} experiment (blue, circle). Also shown are the results from the intermittent measurements with the Møller polarimeter [2, 3] (red, open square). The inner error bars show the statistical uncertainty while the outer error bar is the quadrature sum of the statistical and point-to-point systematic uncertainties. The solid bands show the additional normalization/scale type systematic uncertainty (0.42% Compton and 0.65% Møller). The dashed and solid (green) vertical lines indicate changes at the electron source.

The difference between the triggered and the un-
 triggered counts observed in the DAQ simulation was
 due to DAQ inefficiency. Also, the average DAQ inef-
 ficiency was found to be directly related to the aggregate
 detector rate. These results were used to determine the
 correction to the detector yield for each 1 hr run, based
 on the aggregate detector rate during the run. The DAQ
 inefficiency correction resulted in $< 1\%$ change in the
 extracted polarization. The validity of the corrections and
 the systematic uncertainty due to the corrections (listed
 in Table I) was determined by comparing the polariza-
 tion extracted from triggered vs. un-triggered data over
 a wide range of beam currents (rates) and several differ-
 ent trigger conditions. Thus, the Modelsim simulation
 provided a robust method to determine the inefficiency
 of the DAQ.

Extensive simulation studies provided the comprehen-
 sive list of contributions to the systematic uncertainties,
 tabulated in Table I, with a net systematic uncertainty of
 0.59% for the Compton Polarimeter. The extracted beam
 polarization for the entire second running period of the
 Q_{weak} experiment is shown in Fig. 5. Most of the varia-

TABLE I: Systematic Uncertainties

Source	Uncertainty	$\Delta P/P\%$
Laser Polarization	0.18	0.18
Plane to Plane	secondaries	0.00
magnetic field	0.0011 T	0.13
beam energy	1 MeV	0.08
detector z position	1 mm	0.03
inter plane trigger	1-3 plane	0.19
trigger clustering	1-8 strips	0.01
detector tilt(w.r.t x, y and z)	1 degree	0.06
detector efficiency	0.0 - 1.0	0.1
detector noise	up to 20% of rate	0.1
fringe field	100%	0.05
radiative corrections	20%	0.05
DAQ inefficiency correction	40%	0.3
DAQ inefficiency pt.-to-pt.		0.3
Beam vert. pos. variation	0.5 mrad	0.2
helicity correl. beam pos.	5 nm	< 0.05
helicity correl. beam angle	3 nrad	< 0.05
spin precession in chicane	20 mrad	< 0.03
Total		0.59

tion in the polarization are due to changes at the electron source indicated by the dashed and solid vertical lines. The Compton and Møller measurements [2–4] were quantitatively compared by examining periods of stable polarization. The ratio of Compton to Møller measurements, when averaged over these stable periods using statistical and point-to-point uncertainties, was 1.007 ± 0.003 , to be compared to the total relative normalization uncertainty of 0.77%.

CONCLUSIONS

The polarization of a 1.16 GeV electron beam was measured using a set of diamond micro-strip detectors for the first time. The high resolution of the detectors and their proximity to the primary beam helped record a large fraction of the Compton electron spectrum, spanning both sides of the zero crossing of the Compton asymmetry. These detectors, coupled with a robust analysis technique and rigorous simulations of the polarimeter and the DAQ system, produced a very reliable, high precision measurement of the polarization in a very high radiation environment. They demonstrate that diamond micro-strip detectors are indeed a viable option as tracking detectors, and they are the appropriate choice for tracking detectors that are exposed to very high radiation dose. We have also demonstrated that it is possible

to achieve high precision with a Compton polarimeter operated at beam energies as low as ~ 1 GeV. This has very positive implications for the future PVES program at the upgraded JLab.

ACKNOWLEDGMENTS

This work was funded in part by the U.S. Department of Energy contract # AC05-06OR23177, under which Jefferson Science Associates, LLC operates Thomas Jefferson National Accelerator Facility, and contract # DE-FG02-07ER41528, and by the Natural Sciences and Engineering Research Council of Canada (NSERC). We thank H. Kagan from Ohio State University for teaching us about diamonds, training us on characterizing them and helping us build the proto-type detector.

-
- [1] D. Androic *et al.*, Phys. Rev. Lett. **111**, 121804 (2013).
 - [2] T. Allison *et al.*, Nucl. Instr. Meth. **A781**,105 (2015).
 - [3] M. Hauger, A. Honegger, J. Jourdan, G. Kubon, T. Petitjean, D. Rohe, I. Sick and G. Warren *et al.*, Nucl. Instrum. Meth. A **462**, 382 (2001); J. Magee, Proc. of Sci. PSTP2013, 039 (2013).
 - [4] A. Narayan, Ph. D. Thesis, Mississippi State University, 2015 (unpublished).
 - [5] D. Gustavson *et al.* Nucl. Instr. Meth. **A165**, 177 (1979); L. Knudsen *et al.*, Phys. Lett. **B270**, 97 (1991).
 - [6] D. P. Barber *et al.*, Nucl. Instr. Meth. **A329**, 79 (1993).
 - [7] M. Woods, Proc. of the Workshop on High Energy Polarimeters, Amsterdam, eds. C. W. de Jager *et al.*, p. 843 (1996); SLAC-PUB-7319 (1996).
 - [8] I. Passchier *et al.*, Nucl. Instr. Meth. **A414**, 446 (1998).
 - [9] W. Franklin *et al.*, AIP Conf.Proc. 675, 1058 (2003).
 - [10] M. Baylac *et al.*, Phys. Lett. **B539**, 8 (2002); N. Felletto *et al.*, Nucl. Instr. Meth. **A459**, 412 (2001).
 - [11] A. Acha *et al.* [HAPPEX Collaboration], Phys. Rev. Lett. **98**, 032301 (2007).
 - [12] D. R. Kania, M. I. Landstrass and M. A. Plano, Diam. Relat. Mater. **2**, 1012 (1993).
 - [13] R. Berman (ed), *Physical Properties of Diamond*, Oxford University Press, Oxford, 1965.
 - [14] J. E. Field (ed), *The Properties of Diamond*, Academic, New York, 1979.
 - [15] R. J. Tapper, Rep. Prog. Phys. **63**, 1273 (2000).
 - [16] C. Bauer *et al.* Nucl. Instrum. Methods **367**, 207 (1995).
 - [17] M. M. Zoeller *et al.*, IEEE Trans. Nucl. Sci. **44** 815 (1997).
 - [18] C.K. Sinclair *et al.*, Phys. Rev. ST Accel. Beams **10**, 023501 (2007); P.A. Adderley *et al.*, Phys. Rev. ST Accel. Beams **13**, 010101 (2010).
 - [19] A. Denner and S. Dittmaier, Nucl. Phys.**B540**, 58 (1999).
 - [20] CERN Program Library Long Write-up W5013, Unpublished (1993)
 - [21] Modelsim Reference Manual, Mentor Graphics Corp.,Unpublished (2010).